

Enhanced antitumor efficacy of oncolytic adenovirus-loaded menstrual blood-derived mesenchymal stem cells in combination with peripheral blood mononuclear cells.

Rafael Moreno¹, Carlos Alberto Fajardo¹, Marti Farrera-Sal^{1,2}, Ana Judith Perisé-Barrios³, Alvaro Morales-Molina³, Ahmed Abdullah Al-Zaher¹, Javier García-Castro³, and Ramon Alemany¹.

¹Virotherapy and Gene therapy Group, ProCure Program, Translational Research Laboratory, Instituto Catalan de Oncología-IDIBELL, Barcelona, Spain.

²VCN Biosciences S.L., Grifols Corporate Offices, Sant Cugat del Vallès, Spain.

³Cellular Biotechnology Unit, Institute of Health Carlos III (ISCIII), Majadahonda, Madrid, Spain.

Running title: Antitumor efficacy of oncolytic adenovirus-loaded stem cells.

Keywords: oncolytic adenovirus; mesenchymal stem cells; peripheral blood mononuclear cells; immunotherapy; cancer.

Financial Support

This work was supported by Asociación Española Contra el Cáncer (AECC), BIO2014-57716-C2-1-R grant to R. Alemany and PI14CIII/00005 and PI17CIII/00013 to J.G Castro from the Ministerio de Economía y Competitividad of Spain, Adenonet BIO2015-68990-REDT to R. Alemany from the Ministerio de Economía y Competitividad of Spain, Red ADVANCE(CAT) project COMRDI15-1-0013 to R. Alemany from Ris3CAT and 2014SGR364 research grant to R. Alemany from the ‘Generalitat de Catalunya’. Co-funded by the European Regional Development Fund, a way to Build Europe to R. Alemany.

Corresponding author: Rafael Moreno Olié, IDIBELL-Institut Català d'Oncologia, Av Gran Via de l'Hospitalet 199-203, L'Hospitalet de Llobregat, 08907 Barcelona, Spain. Phone: 34-9326-072-52; Fax: 34-9326-074-66; E-mail: rafamoreno@iconcologia.net

Disclosure of Potential Conflicts of Interest: No potential conflicts of interest are disclosed.

ABSTRACT

Several studies have evaluated the efficacy of using human oncolytic adenovirus-loaded mesenchymal stem cells for cancer treatment. For example, we have described the antitumor efficacy of CELYVIR, autologous bone marrow mesenchymal stem cells infected with the oncolytic adenovirus ICOVIR-5, for treatment of neuroblastoma patients. Results from this clinical trial point out the role of the immune system in the clinical outcome. In this context, a better understanding of the immunophenotypic changes of human mesenchymal stem cells upon adenoviral infection and how these changes affect human autologous or allogeneic peripheral blood mononuclear cells (PBMCs) could guide strategies to improve the antitumor efficacy of infected Mesenchymal Stem Cells (MSCs). In this work, we show how infection by an oncolytic adenovirus (OAdv) induces Toll-like receptor 9 overexpression and activation of the NF- κ B pathway in menstrual blood-derived mesenchymal stem cells (MenSCs), leading to a specific cytokine secretion profile. Moreover, a pro-inflammatory environment, mainly mediated by monocyte activation that leads to the activation of both T-cells and natural killer cells (NK cells), is generated when OAdv-loaded MenSCs are co-cultured with allogeneic PBMCs. This combination of allogeneic PBMCs and OAdv-loaded MenSCs enhances antitumor efficacy both *in vitro* and *in vivo*, an effect partially mediated monocytes and NK cells. Altogether our results demonstrate not only the importance of the immune system for the oncolytic adenovirus-loaded MSCs antitumor efficacy, but in particular the benefits of using allogeneic MSCs for this therapy.

INTRODUCTION

Among the variety of strategies designed to improve the limited antitumor efficacy observed after systemic oncolytic adenovirus (OAdv) administration in clinical trials, the use of mesenchymal stem cells (MSCs) as cell carriers for oncolytic adenovirus is of special interest because of their natural tumor tropism (1) and immunomodulatory properties (2). In the last decades, we and others have studied the use of MSCs as cell carriers for oncolytic adenoviruses. In this context, CELYVIR, a therapeutic approach exploiting the use of autologous human bone marrow-derived MSCs as cell carriers for the oncolytic adenovirus ICOVIR5, has been evaluated in clinical studies for pediatric refractory metastatic neuroblastoma treatment (NTC01844661). Results from this clinical trial demonstrated tolerance to the treatment and clinical responses including complete remissions (3,4). The activation status of the immune system of the patients and the inflammatory profile of the MSCs were suggested to play a role in treatment outcome (4). Recently, a dog version of CELYVIR consisting in the combination of dog healthy allogeneic MSCs infected with a canine oncolytic adenovirus has been evaluated in a clinical study to treat spontaneous canine tumor (5). A 74% response rate was determined in the assay with 14.8% showing complete responses, including total remissions of lung metastasis. Interestingly, microenvironment alterations and immune cell infiltration in tumor after treatment were observed. Altogether, these clinical data pointed out the main role of the immune system for OAdv-loaded MSCs antitumor efficacy although more experimental evidences are needed to better understand the immune mechanisms involved in the antitumor efficacy of CELYVIR.

The immunosuppressive properties of mesenchymal stem cells have been extensively reported (2,6,7). However, in 2010, the group of Aline Betancourt introduced a new paradigm for MSCs: their polarization into a pro-inflammatory MSC1 or an immunosuppressive MSC2 phenotype

(8,9), with a clear impact on tumor growth (10). More recently it has been reviewed how pathogen-associated molecular patterns (PAMPS) modulate MSCs immunophenotype by signaling through Toll-like Receptors (TLRs), including the activation of TLR-3 by poly(I:C), TLR-4 by Lipopolysaccharide (LPS) or TLR-9 by non-methylated CpG sequence (11,12). Recognition of unmethylated CpG motifs from adenovirus double-stranded DNA by dendritic cells' TLR-9 leads to their maturation and induces transcriptional activation of pro-inflammatory cytokines and inflammasome components (13). Thus, although it has not been demonstrated for human mesenchymal stem cells, it is plausible to hypothesize that adenoviral infection could switch the immune-phenotype of MSCs toward a pro-inflammatory status through the activation of TLR-9.

Systemic administration of OAdv-loaded mesenchymal stem cells has been used in several animal models (14-18). However, the animal models used to date limit the study of pro-inflammatory status of MSCs after OAdv infection and its effect on tumor growth. On one hand, immunodeficient mice bearing human xenograft tumors lack a complete immune system and pro-inflammatory responses. On the other hand, human adenoviruses show species-specific replication, thus limiting the study of oncolysis and antitumor immune responses in immunocompetent mice.

We have recently described the advantages of using menstrual blood-derived mesenchymal stem cells (MenSCs) as an alternative to bone-marrow mesenchymal stem cells as cell carriers for OAdv (19). In this follow-up study, we sought to assess the antitumor efficacy of OAdv infected human menstrual blood-derived mesenchymal stem cells in the presence of autologous and allogeneic human peripheral blood mononuclear cells (PBMCs). We show that infection by OAdv induces MenSCs immunophenotypic profile changes, generating a pro-inflammatory environment in co-cultures with allogeneic PBMCs, mainly mediated by monocyte activation,

and resulting in the activation of both T-cells and Natural Killer cells (NK cells). Finally, we demonstrate that combination of allogeneic PBMCs and OAdv-loaded MenSCs present an enhanced antitumor efficacy both *in vitro* and *in vivo*, with monocytes and NK cells playing an important role in this efficacy.

MATERIALS AND METHODS

Cell culture

The cancer cell lines A549 (human lung adenocarcinoma), A431 (epidermoid carcinoma), FaDu (pharynx squamous cell carcinoma) and HEK-293 (human embryonic kidney) were obtained and authenticated by STR profiling by the American Type Culture Collection (ATCC, Manassas, VA). All tumor cell lines were maintained with Dulbecco's Modified Eagle's Medium supplemented with 5 or 10% fetal bovine serum and 1% penicillin/streptomycin (Life Technologies, Carlsbad, CA, USA) at 37°C, 5% CO₂. Cell lines were routinely tested for mycoplasma presence. The A431-GL and FaDu-GL cell line was generated by sorting of A431 and FaDu cells previously transduced with a lentiviral vector encoding GFP and luciferase. Isolation and characterization of MenSCs has been previously described (19). Although different MenSCs passages were used through the different experiments (based on sample availability), the same cell passage from different donors was always used for each experiment, being 5 the highest passage used.

All experiments employing human PBMCs were approved by the ethics committees of the University Hospital of Bellvitge and the Blood and Tissue Bank (BST) from Catalonia. PBMCs of healthy donors were isolated from the blood by ficoll (Rafer, Spain) density gradient centrifugation in Leucosep tubes (Greiner Bio-one, Kremsmünster, Austria) following manufacturer's recommendations. NK- or monocyte-depleted PBMCs were generated using

human CD56 or CD14 microbeads respectively, LD columns and MidiMACS separator (all from MiltenyiBiotec, BergischGladbach, Germany).

Oncolytic adenovirus

The oncolytic adenovirus used though this work has been ICOVIR15, previously described by our group (20).

Flow cytometry analysis of Toll-like receptor 9

MenSCs (1×10^5 cells/sample) from 3 different donors (passage 3) were infected with ICOVIR15 at 50 TU/cell. After 24h, cells were analyzed by flow cytometry for expression of TLR-9. Allophycocyanin (APC)-conjugated antibody against TLR9 (Thermo Fisher Scientific, Waltham, MA USA, clone eB72-1665) was used. A Gallios cytometer (Beckman Coulter, Brea, CA, USA) was used and 10,000 events were analyzed for each sample. FlowJo v7.6.5 (Tree Star, Inc., San Carlos, CA, USA) software was used for the analysis of the data.

NF- κ B reporter luciferase assay

1×10^5 MenSCs (passage 2) were transduced for 16h with the non-replicative lentiviral vector pHAGE-NF κ B-TA-LUC-UBS-GFP-W (kindly provided by Dr. García-Castro, Addgene plasmid #49343) at a multiplicity of infection (MOI) of 2. This lentiviral vector encodes the NF- κ B consensus binding sequence upstream of the minimal TA promoter of herpes simplex virus followed by the firefly luciferase and GFP genes under the control of the ubiquitin-C promoter. Transduced MenSCs were infected with ICOVIR15 at 50 TU/cell, and luciferase activity from cell lysis was determined at different time-points post-infection using the luciferase assay system (Promega Corporation, Madison, WI, USA).

Cytokine array and Luminex quantification

1×10^6 MenSCs (passage 3) were infected with ICOVIR15 at 50 TU/cell in duplicate. After 48h,

the supernatant from infected or uninfected MenSCs was collected and the secreted cytokine profile was evaluated using two different analysis: the Proteome Profiler Human Cytokine Array Kit (R&D; Minneapolis, MN, USA) and the Th1/Th2/Th9/Th17/Th22/Treg Cytokine 18-Plex Human ProcartaPlex Panel (Thermo Fisher Scientific). For the former, cytokine quantification was determined by estimating the spot integrated density using the ImageLab software (Bio-Rad Laboratories, Hercules, CA, USA). For the Cytokine Array using the multiplexing unit MAGPIX (Luminex Corporation, Austin, TX, USA) and the ProcartaPlex Analyst software (Thermo Fisher Scientific) for the ProcartaPlex Panel.

Enzyme-linked immunosorbent assay (ELISA)

MenSCs (2.5×10^5 cells per well in 6-well plaques) from 3 different donors (passage 3) were infected with ICOVIR15 at an MOI of 50 for 24h. The next day, PBMCs from the same donors or from an allogeneic donor were isolated using ficoll gradient centrifugation. Autologous or allogeneic PBMCs (2.5×10^6 PBMCs) were co-cultured with infected or uninfected MenSCs (PBMCs:MenSCs = 10). After 48h of incubation, co-culture supernatants were collected and cytokine level was assessed with the human IFN- γ , TNF- α (Peprotech, Rocky Hill, NJ, USA), IL-2 (Biolegend) or IFN- α (Mabtech AB, Nacka Strand Sweden) ELISA kits according to the manufacturer's instructions.

Flow cytometry analysis of PBMCs cell activation.

For the T-cells and NK cells activation assay, MenSCs from 3 different donors (passage 4) were infected with ICOVIR15 at a MOI of 50 for 24h. The next day, PBMCs from autologous and one allogeneic donor were isolated and co-cultured directly in contact or using a transwell system with infected or un-infected MenSCs (PBMCs-to-MenSCs ration of 10) in triplicate. After 48h of co-culture, PBMCs were harvested, stained for cell viability with LIVE/DEAD

Green (Thermo Fisher Scientific), divided into two different samples followed by incubation with: panel 1 (T-cell activation) and panel 2 (NK cell activation) (see supplementary Material and Methods for antibodies details). A Gallios cytometer was used and 20,000 live lymphocytes were analyzed for each sample.

***In vitro* cytotoxicity assay**

MenSCs (passage 4) were infected with ICOVIR15 at MOI 50 for 24h. The next day, PBMCs from an allogeneic donor were isolated using ficoll gradient centrifugation. Infected or uninfected MenSCs, allogeneic PBMCs and tumoral cells expressing GFP protein (A431-GL or FaDu-GL) were co-cultured in 24-well plates at the following cell density (in triplicates): MenSCs (infected or un-infected) 2×10^3 cells/cm², A431-GL 1×10^4 cells/cm², FaDu-GL 5×10^3 cells/cm², allogeneic PBMCs at 10:1 ratio with respect to tumor cells (1×10^5 or 5×10^4 cells/cm² when A431-GL or FaDu-GL were present respectively). After 5 days in co-culture, viable GFP-expressing tumoral cells were determined by flow cytometry (negative for LIVE/DEAD and positive for GFP). CountBright absolute counting beads (Thermo Fisher Scientific) were used for absolute cell number determination. Cytotoxicity was expressed as the percentage of live cancer cells in co-cultures normalized to that of cancer cells cultured alone.

***In vivo* oncolytic adenovirus tumor delivery and antitumor efficacy**

In vivo studies were performed at the ICO-IDIBELL animal facility (Barcelona, Spain) AAALAC unit 1155, and approved by IDIBELL's Ethical Committee for Animal Experimentation.

Athymic nu/nu mice

Lung adenocarcinoma xenograft tumors were established by implanting 5×10^6 A549 cells subcutaneously into both flanks of 8-week-old female Athymic nu/nu mice. When tumors reached 100-120 mm³, mice were randomized and distributed into groups. To evaluate systemic

efficacy, animals were treated with a single intraperitoneal dose of PBS or 5×10^{10} vp/mice of OAdv (ICOVIR15), MenSCs (4×10^6 cells) or MenSC/OAdv (4×10^6 cells previously infected with ICOVIR15 at MOI 50 for 24h).

NOD scid gamma (NSG) mice

The same tumor model was established but in this case implanting 5×10^6 A549 or A431 cells suspended in a 100 μ L PBS and Matrigel mixture (1:1, v/v; BD biosciences) into both flanks of 8-week-old NSG mice. When tumors reached 100-120 mm³, mice were randomized and distributed into the following groups: allogeneic PBMCs + PBS; MenSCs; OAdv or MenSCs/OAdv (MenSCs previously infected with ICOVIR15 at MOI 50 for 24h) and MenSCs/OAdv without allogeneic PBMCs (only for the A549 experiment). To evaluate antitumor efficacy, 1×10^7 human allogeneic PBMCs were administered to the mice by intravenous injection except animals receiving only MenSCs/OAdv. The next day, animals were treated with a single intraperitoneal dose of PBS, 1×10^{10} vp/mice of OAdv (ICOVIR15), 5×10^6 MenSCs or 5×10^6 MenSCs/OAdv.

Tumor volume was calculated according to the equation $V(\text{mm}^3) = \pi/6 \times W^2 \times L$, where W and L are the width and the length of the tumor, respectively. Data are expressed as the tumor size relative to the size at the beginning of the therapy (tumor growth). At the end of the study, animals were euthanized and tumors were collected. One half was frozen for DNA extraction, and the other half was fixed in 4% formaldehyde for 24h and embedded in paraffin.

For the antitumor efficacy studies involving monocytes and NK cell-depleted allogeneic PBMCs, the same animal and tumor model were used. When A549 tumors reached 100-120 mm³, mice were randomized and distributed into the following groups: allogeneic PBMCs + PBS or MenSCs/OAdv, allogeneic PBMCs depleted for monocytes + MenSCs/OAdv and allogeneic PBMCs depleted for NK cells + MenSCs/OAdv. PBMCs from a single donor were

isolated, and a part of the sample was depleted for monocytes or NK cells as described above. Monocytes and NK-depletion was confirmed by flow cytometry after staining of the cells with LIVE/DEAD violet, and APC-CD14 or PE-CD56. Finally, 1×10^7 human allogeneic PBMCs, human allogeneic monocytes-depleted PBMCs or human allogeneic NK-depleted PBMCs were administered to the mice by intravenous injection. Next day, animals were treated with a single intraperitoneal dose of PBS or 5×10^6 MenSCs/OAd and tumor size was monitored as previously described.

Determination of adenoviral genomes in tumor samples

A549 frozen tumor samples were mechanically homogenized and total DNA was extracted following the QIAamp DNA Mini Kit (QIAGEN, Valencia, CA) protocol for tissue DNA Purification. Adenoviral genome copies were quantified in triplicate by Quantitative Real Time-PCR using the specific set of primers targeting the hexon sequence (forward 5'-CTT CGA TGA TGC CGC AGT G-3', reverse 5'-ATG AAC CGC AGC GTC AAA CG-3'). PCR conditions were: 95°C 10 minutes, 40x cycles of 95°C 15 seconds, 60°C 1 minute and 72°C 7 seconds. Real Time PCR was performed using LightCycler 480 SYBR Green I Master (Roche). Adenoviral genome copy numbers were calculated using a standard curve of serially diluted pAd5wt, a plasmid containing the complete Adenoviral type 5 genome and for which the genome copy number was known.

Histology and immunohistochemistry

A549 paraffin-embedded sections (5- μ m thickness) of tumors samples were treated with an anti-Ad2/5E1A antibody (SC-430, Santa Cruz, Dallas, TX, USA) as primary antibody diluted 1/200 in PBS. Immunohistochemical staining was performed with EnVision (DAKO, Hamburg, Germany), according to manufactures' instructions, and with hematoxylin and eosin. Images

were acquired using the Nikon Eclipse 80i microscope running NIS elements BR software (Nikon Instruments Europe BV, Amsterdam, Netherlands).

Statistical analysis

Statistical comparisons between two groups were performed using the Mann-Whitney U test (2-tailed). For comparison of more than two groups, Kruskal-Wallis with Dunn *post-hoc* test was used. Statistical significance was established as $p < 0.05$. Data are presented as the mean \pm SD or SEM. All statistical analysis were calculated with GraphPad Prism software.

RESULTS

Immunophenotypic profile changes in MenSCs after OAdv infection

Adenoviral infection has been described as triggering the expression of TLR-9 in different cell types (21,22). We therefore decided to evaluate the expression of TLR9 on MenSCs in response to OAdv infection. 24h after OAdv infection, the percentage of MenSCs expressing TLR9 was significantly increased 1.46-fold (Figure 1A). We next studied the activation of NF- κ B pathway in MenSCs after OAdv infection. For this, MenSCs were transduced with a lentiviral vector containing a NF- κ B promoter-driven luciferase reporter system for detecting NF- κ B activation (23), and luciferase expression was evaluated at different time points after OAdv infection. Significant expression of luciferase was observed 24h post-infection (Figure 1B), indicating an activation of the NF- κ B pathway after OAdv infection.

To determine whether OAdv-induced NF- κ B activation triggers the expression of immune response genes, we evaluated the production of several pro-inflammatory and immune-related cytokines in uninfected or OAdv-infected MenSCs after 48h of infection using both, a cytokine array and a Luminex assay. From the 36 cytokines quantified in the cytokine array

(supplementary Fig.1), only macrophage migration inhibitory factor (MIF), IL-8 and Serpin E1 could be detected, and all three were overexpressed after OAd infection (fold-increase of 1.79, 2.27 and 9.01, respectively) (Figure 1C). Results from the 19 cytokines evaluated with the Luminex assay confirmed the overexpression of IL-8 (fold-increase of 1.29), and revealed a slight increase in the expression of IL-9, IL-18 and IL-21 after virus infection (Figure 1D).

By knocking down the TLR-9 expression on MenSCs using a lentivirus coding for a short hairpin-RNA against the human TLR-9, we confirmed the role of the receptor on the NF- κ B pathway activation and cytokines expression after OAdv infection (supplementary figure 2).

In summary, these results indicate an increase in the secretion profile of specific pro-inflammatory cytokines in response to the NF- κ B pathway activation in MenSCs after OAdv infection, as a result the activation of TLR-9 by viral genome.

OAdv infected MenSCs stimulate a pro-inflammatory environment in co-culture with allogeneic PBMCs.

To evaluate if OAdv-loaded MenSCs have an effect on the immunological status of PBMCs, we first analyzed the expression of several pro-inflammatory cytokines from autologous or allogeneic human PBMCs co-cultured with uninfected or OAdv-infected MenSCs for 48h. Uninfected MenSCs, independently from the source of the PBMCs, and infected MenSCs in co-culture with autologous PBMCs had no significant effect on the secretion of cytokines by PBMCs (Figure 2). However, a significant increase in the expression level of all four cytokines evaluated was observed when human allogeneic PBMCs were co-cultured in the presence of OAd-infected MenSCs, indicating the induction of a pro-inflammatory environment in the co-culture. In order to determine the contribution of different cell subtypes in the induction of this

pro-inflammatory environment, infected or uninfected MenSCs were cultured in the presence of allogeneic PBMCs from which monocytes, NK cells, or both were previously depleted. We found that the depletion of monocytes in the co-culture significantly decreased the level of all four cytokines indicating their importance in establishing the pro-inflammatory environment (Figure 3).

To evaluate if this pro-inflammatory environment triggers the activation of the different cell subtypes in PBMCs, we further investigated the activation of autologous and allogeneic CD4⁺ T cells, CD8⁺ T cells and NK cells in co-culture with infected or uninfected MenSCs. As shown in Fig.4A, pro-inflammatory cytokines secreted by the co-culture of human allogeneic PBMCs and OAd-infected MenSCs induced CD8⁺ and CD4⁺ T-cell activation as indicated by an increase in the expression of the activation markers CD69 in both cell lines, and CD25 in CD4⁺ T-cell in response not only to the presence of the virus but also in the use of allogeneic PBMCs. Similarly, the percentage and intensity of NK cells (CD56⁺CD16⁺) expressing the activation marker CD69 was significantly higher when allogeneic PBMCs were co-cultured with OAd-infected MenSCs (Figure 4B). Moreover, the percentage and intensity of NK cells expressing the degranulation marker CD107a was significantly higher when OAd-infected MenSCs were co-cultured not only with allogeneic but also with autologous PBMCs, probably indicating the effect of the OAdv on NK activation. To confirm that secreted factors from OAdv-infected MenSCs induce the observed T-cells and NK-cell activation, a similar experiment was carried out but including a transwell assay to separate PBMCs from infected MenSCs. Thus, CD69 upregulation was measured and compared on CD8⁺, CD4⁺ or CD56⁺CD16⁺ cells employing direct contact cell-to-cell or transwell co-culture assays. As shown in figure 4C, whereas a similar and significant CD69 upregulation was detected for all cell types evaluated independently of the co-culture conditions (direct cell-to-cell contact or using transwells), no differences were determined

between the co-culture methodology used. This result points out the role of the soluble factor secreted by OAdv-secreted MenSCs on cell activation.

Overall these findings demonstrate that co-culture of allogeneic PBMCs and OAdv-loaded MenSCs induce a pro-inflammatory environment mediated in part by monocytes, which results in the activation of CD8⁺, CD4⁺ T-cell and NK cells.

Allogeneic PBMCs enhance the antitumor efficacy of OAdv-loaded MenSCs *in vitro*.

We next addressed if allogeneic PBMCs could increase the antitumor efficacy of OAdv-infected MenSCs *in vitro*. For this, two different GFP-expressing cancer cell lines (A431-GL and FaDu-GL, both of them considered partly resistant to adenovirus infection) were co-cultured with OAdv-infected or uninfected MenSCs in the presence or absence of allogeneic PBMCs for 5 days, and the percentage of cancer cell death was determined by flow cytometry. The combination of allogeneic PBMCs and OAdv loaded MenSCs showed increased antitumor efficacy compared to OAdv-infected MenSCs alone or uninfected MenSCs in combination with allogeneic PBMCs (Figure 5).

Allogeneic human PBMCs increase the antitumor efficacy of OAdv-loaded MenSCs *in vivo*

We recently reported the tumor homing properties of MenSCs/OAdv after systemic administration in human tumor-bearing athymic nu/nu mice (19), but the antitumor efficacy of this strategy was not evaluated. We therefore evaluated the antitumor efficacy of OAdv-loaded MenSCs in A549-tumor bearing nude mice. In contrast to the treatment with OAd alone, in which tumor growth was significantly controlled, OAdv-loaded MenSCs showed only moderate antitumor efficacy (Figure 6A). These results suggest that although MenSCs migrated to the tumors after systemic administration, the amount of cells arriving at and the number of virus

particles delivered to the tumors during the first days after treatment was not enough to control tumor growth. Nevertheless, the total viral genomes detected in tumors at the end of the experiment were similar to the OAdv group. This apparently contradiction could be explained considering that the OAdv content in tumor at early stages of the experiment determines the antitumor efficacy at later stages. Thus, directly administrated OAdv leads to a larger amount of initial virus in the tumor that is able to control tumor growth but also depletes the substrate (tumor cells) faster. Tumors develop fibroblast barriers, which do not allow the efficient spread of the virus, and these barriers form isolated tumor nodules that eventually grow without virus. At the end of the experiments the tumors analyzed contained few virus despite their lower size. However, for the MenSCs/OAdv group, since the initial amount of virus in the tumor is lower, the scarce amount of foci of replicating virus cannot eliminate all the tumor cells in these fast-growing tumor models and there is no apparent antitumor efficacy but as the permissive substrate (tumor cells) is not eliminated, the virus is amplified progressively until the end of the experiment. .

Since the above-described *in vitro* characterization strongly suggests an important role of MenSC/OAdv in modulating the antitumor immune response of allogeneic PBMCs, we hypothesized that the *in vivo* antitumor efficacy of MenSC/OAdv could be improved in the presence of human immune cells. We decided to use the immunodeficient mouse model NSG with human tumors and human PBMCs, a model previously used to evaluate the combination of human adenovirus and human PBMCs (24,25).

Thus, NSG mice bearing subcutaneous A549 tumors received an intravenous injection of 10^7 human allogeneic PBMCs. The next day, mice received a single intraperitoneal injection of PBS, OAdv (ICOVIR15), MenSCs or MenSC/OAdv. A group consisting of mice treated with MenSC/OAdv in the absence of human allogeneic PBMCs was also included to specifically

evaluate the effect of the human allogeneic PBMCs on the MenSC/OAdv antitumor activity. To simplify the experiment, and taking into account our previous result where human PBMCs had no effect on tumor growth (24), we did not evaluate the rest of the groups in the absence of human PBMCs. As shown in figure 6B, antitumor efficacy could be detected only when OAdv-loaded MenSCs were combined with the administration of allogeneic PBMCs, pointing out the relevance of allogeneic PBMCs in the antitumor effect. Importantly, there were no differences in the viral load in the tumors at the end of the experiment among MenSCs OAdv-loaded groups in the presence or absence of human allogeneic PBMCs, indicating that PBMCs did not interfere with MenSCs/OAdv tumor homing. A visual not quantitative analysis of diverse IHC images from each group was performed to confirm the presence of OAdv in the tumors. Histology of the tumors at the end of the experiment revealed the expression of the E1a protein in tumors of animals treated with the oncolytic adenovirus alone or in combination with MenSCs, confirming the correct OAdv delivery and amplification in tumors. We also tested the antitumor efficacy of the different groups in the presence of human allogeneic PBMCs in a second tumor model, NSG mice bearing subcutaneously A431 tumors and transferred with human PBMCs. As show in the figure 6C, a significant tumor growth control was observed only for the MenSCs/OAdv treated group, although it was restricted to early days after treatment (from day 3 to day 8). However, this result is of special interest since A431 are partly resistant to adenovirus infection strongly suggesting the effect of the allogeneic PBMCs on the efficacy observed since low or no viral replication is expected in this tumoral cells.

Effect of monocytes or NK cells depletion on antitumor activity of OAdv-loaded MenSCs *in vivo*

Finally, having demonstrated the importance of monocytes in establishing the pro-inflammatory environment, and the NK cell activation *in vitro* after allogeneic PBMCs and OAdv-loaded MenSCs co-culture, we next evaluated the influence of these cell types on the antitumor efficacy observed *in vivo*. NSG mice bearing subcutaneous A549 tumors received an intravenous injection of 10^7 human allogeneic PBMCs, 10^7 monocytes-depleted human allogeneic PBMCs (PBMCs-Mo⁻) or 10^7 NK-depleted human allogeneic PBMCs (PBMCs-NK⁻). 24h later, mice received a single intraperitoneally administration of PBS or 5×10^6 MenSCs/OAdv. As show in the figure 6D, a significant tumor growth control was observed only when a complete PBMCs administration was done. These differences were significant against both, the monocyte and NK cell depleted groups, although it was restricted to early days after treatment (from day 3 to day 8). Nevertheless, at the end of the experiment the group transferred with fully PBMCs showed 1.5 and 1.6-fold decrease (($p=0.066$ and 0.057) in the percentage of tumor growth compared to groups depleted for NK cells and monocytes respectively. We consider that these results support the hypothesis of the role of the innate response on the tumor control efficacy observed for OAdv-loaded MenSCs treatment.

DISCUSSION

In the present work we evaluated the effect of OAd infection on MenSCs at the level of their immune profile, their behavior in the presence of autologous or allogeneic human PBMCs, and their impact in antitumor efficacy *in vitro* and *in vivo*. We show that adenovirus infection of MenSCs increases the expression of TLR-9, leading to NF- κ B pathway activation. We also detected an increase in the expression of diverse proinflammatory cytokines, including macrophage migration inhibitory factor, an upstream activator of innate immunity (26), IL-8, a

proinflammatory cytokine also overexpressed in MSCs after TLR-3 and TLR-4 stimulation (27), and Serpin E1, which stimulates macrophage activation through TLR signaling (28), among others. These results are in agreement with studies evaluating adenovirus infection of dendritic cells showing that, during endosomal trafficking, Ad5 virions are accumulated in the late endosomal compartment where they are fused with vesicles carrying TLR-9 (22). This receptor recognizes unmethylated CpG motifs in the adenovirus double-stranded DNA, leading to transcriptional activation of pro-inflammatory cytokine and inflammasome-related genes via NF κ B and AP-1 signaling pathways (29,30). Moreover, taking into account the multiple mechanisms used by mesenchymal stem cells to modulate the immune system, we cannot discard additional immunophenotypic changes on MenSCs after OAdv infection than those evaluated in this work. Altogether our results confirm that adenovirus infection alters the immune status of MenSCs towards a more proinflammatory profile, as a result of OAd-mediated stimulation of TLR-9, as described for other MSCs' TLR stimulation (9).

We further evaluated the effect of this adenovirus-specific MenSCs immune profile on the activation of the immune system *in vitro*. A clear pro-inflammatory environment was detected when infected MenSCs were co-cultured with allogeneic, but not with autologous, PBMCs. Pro-inflammatory cytokines were highly expressed (IFN- γ , TNF- α , IL-2, and IFN- α) in these co-culture conditions, mainly mediated by monocyte activation and probably in response to the presence of adenovirus as previously described (31,32). Interestingly, this pro-inflammatory environment was, in part, independent of cell contact but related to soluble factors secreted by infected MenSCs. Moreover, this pro-inflammatory environment led to CD8⁺ and CD4⁺ T-cell activation as indicated by an increase in the expression of CD69 and CD25, in response not only to the presence of the virus but also to the HLA mismatch between the CD4⁺ T-cell and MenSCs.

Different studies have recently pointed out the capacity of oncolytic virotherapy to promote intratumoral T-cell infiltration and enhance checkpoint inhibitor immunotherapy (33,34), therefore it is plausible to expect a similar effect for OAdv-infected MenSCs. NK cell activation was also detected when infected MenSCs were co-cultured with allogeneic PBMCs as shown by the expression of CD69 and CD107a. These results are in agreement with a previous study in which oncolytic reovirus infection stimulate monocytes to secrete IFN- α , resulting in NK cell activation and improved antitumor efficacy (35).

A greater antitumor potency of OAd-loaded MenSCs and allogeneic PBMCs combination was confirmed not only *in vitro* (evaluated in FaDu and A431 cell lines, partly resistant to adenovirus infection (36,37)), but most importantly *in vivo*. In this work, we demonstrate for the first time the antitumor efficacy of OAdv-loaded MSCs after only a single systemic administration, indicating that this antitumor efficacy is mediated by the presence of allogeneic PBMCs. Moreover, when NK cells are depleted from PBMCs transferred to mice, antitumor efficacy is lost, indicating the important role of NK cells in the antitumor efficacy exerted by OAdv-loaded MSCs. A similar lack of antitumor efficacy was observed with monocyte-depleted PBMCs as expected according to the role described for monocytes on NK cell activation (38,39) and our own *in vitro* results. Finally, it is worth mentioning the limitation of our model in which only innate immune responses can be studied since no adaptive responses are generated in this mouse model. Thus, this model is likely underestimating the overall antitumor efficacy since recent evidence suggest that NK cells can act as initiators of adaptive immune response (reviewed in (40)).

In summary, our work describes the immune-stimulatory properties of allogeneic MenSCs infected with oncolytic adenoviruses and their potential benefits as an alternative to the conventional autologous MSCs used in the CELYVIR clinical trials. In this regard, the clinical

benefits using OAdv-infected allogeneic MSCs to treat canine tumors also support the use of healthy allogeneic donor MSCs instead of autologous MSCs (5). Interestingly, in this study there was no correlation between the gender of the MSCs donor or patient and the efficacy observed, indicating that OAdv-loaded MSCs could be a potential treatment not only for female but also for male patients. Thus, to create a homogenous and well characterized allogeneic MSCs master bank from allogeneic healthy donors, should be considered for the future development of CELYVIR. MenSCs have been extensively characterized *in vitro* and *in vivo* and their potential for cellular therapy has been described (41-43), pointing out that menstrual blood represents an efficient and ethically accepted source of MSCs, and could be considered to generate this MSCs master bank. Finally, data accumulated from patients, dogs and preclinical assays (including the present work) strongly suggest the role of the immune system status in the outcome of the therapy. Although a specific predictive marker has still not been found, assessing the patient immune system and the capability of OAd-loaded MSCs from different donors to activate patients PBMCs could serve as a biomarker for therapy outcome.

From here on, another important factor in improving the efficacy of CELYVIR should be the optimization of the oncolytic adenovirus used by, for example, using more potent oncolytic adenoviruses (44) or oncolytic adenoviruses encoding immunostimulatory sequences or transgenes to enhance the immune response against the tumor (24,45,46).

ACKNOWLEDGMENTS

The authors thank Jana de Sostoa, Dolores Ramos and Silvia Torres for their lab technical support. We also thank Vanessa Cervera for samples processing. We are grateful to Ashleigh Jones for grammatical and style proofreading.

REFERENCES

1. Uchibori R, Tsukahara T, Ohmine K, Ozawa K. Cancer gene therapy using mesenchymal stem cells. *International journal of hematology* **2014**;99(4):377-82.
2. Najar M, Raicevic G, Crompton E, Fayyad-Kazan H, Bron D, Toungouz M, *et al.* The Immunomodulatory Potential of Mesenchymal Stromal Cells: A Story of a Regulatory Network. *Journal of immunotherapy* **2016**;39(2):45-59.
3. Garcia-Castro J, Alemany R, Cascallo M, Martinez-Quintanilla J, Arriero Mdel M, Lassaletta A, *et al.* Treatment of metastatic neuroblastoma with systemic oncolytic virotherapy delivered by autologous mesenchymal stem cells: an exploratory study. *Cancer gene therapy* **2010**;17(7):476-83.
4. Melen GJ, Franco-Luzon L, Ruano D, Gonzalez-Murillo A, Alfranca A, Casco F, *et al.* Influence of carrier cells on the clinical outcome of children with neuroblastoma treated with high dose of oncolytic adenovirus delivered in mesenchymal stem cells. *Cancer letters* **2016**;371(2):161-70.
5. Cejalvo T, Perise-Barrios AJ, Portillo ID, Laborda E, Rodriguez-Milla MA, Cubillo I, *et al.* Remission of spontaneous canine tumors after systemic cellular viroimmunotherapy. *Cancer research* **2018**.
6. Gebler A, Zabel O, Seliger B. The immunomodulatory capacity of mesenchymal stem cells. *Trends in molecular medicine* **2012**;18(2):128-34.
7. Najar M, Raicevic G, Fayyad-Kazan H, Bron D, Toungouz M, Lagneaux L. Mesenchymal stromal cells and immunomodulation: A gathering of regulatory immune cells. *Cytotherapy* **2016**;18(2):160-71.
8. Bunnell BA, Betancourt AM, Sullivan DE. New concepts on the immune modulation mediated by mesenchymal stem cells. *Stem cell research & therapy* **2010**;1(5):34.
9. Waterman RS, Tomchuck SL, Henkle SL, Betancourt AM. A new mesenchymal stem cell (MSC) paradigm: polarization into a pro-inflammatory MSC1 or an Immunosuppressive MSC2 phenotype. *PloS one* **2010**;5(4):e10088.
10. Waterman RS, Henkle SL, Betancourt AM. Mesenchymal stem cell 1 (MSC1)-based therapy attenuates tumor growth whereas MSC2-treatment promotes tumor growth and metastasis. *PloS one* **2012**;7(9):e45590.
11. Najar M, Krayem M, Meuleman N, Bron D, Lagneaux L. Mesenchymal Stromal Cells and Toll-Like Receptor Priming: A Critical Review. *Immune network* **2017**;17(2):89-102.
12. Sangiorgi B, Panepucci RA. Modulation of Immunoregulatory Properties of Mesenchymal Stromal Cells by Toll-Like Receptors: Potential Applications on GVHD. *Stem cells international* **2016**;2016:9434250.
13. Eichholz K, Bru T, Tran TT, Fernandes P, Welles H, Mennechet FJ, *et al.* Immune-Complexed Adenovirus Induce AIM2-Mediated Pyroptosis in Human Dendritic Cells. *PLoS pathogens* **2016**;12(9):e1005871.
14. Alfano AL, Nicola Candia A, Cuneo N, Guttlein LN, Soderini A, Rotondaro C, *et al.* Oncolytic Adenovirus-Loaded Menstrual Blood Stem Cells Overcome the Blockade of Viral Activity Exerted by Ovarian Cancer Ascites. *Molecular therapy oncolytics* **2017**;6:31-44.
15. Hakkarainen T, Sarkioja M, Lehenkari P, Miettinen S, Ylikomi T, Suuronen R, *et al.* Human mesenchymal stem cells lack tumor tropism but enhance the antitumor activity of oncolytic adenoviruses in orthotopic lung and breast tumors. *Human gene therapy* **2007**;18(7):627-41.
16. Kidd S, Caldwell L, Dietrich M, Samudio I, Spaeth EL, Watson K, *et al.* Mesenchymal stromal cells alone or expressing interferon-beta suppress pancreatic tumors in vivo, an effect countered by anti-inflammatory treatment. *Cytotherapy* **2010**;12(5):615-25.

17. Rincon E, Cejalvo T, Kanojia D, Alfranca A, Rodriguez-Milla MA, Gil Hoyos RA, *et al.* Mesenchymal stem cell carriers enhance antitumor efficacy of oncolytic adenoviruses in an immunocompetent mouse model. *Oncotarget* **2017**;8(28):45415-31.
18. Yuan X, Zhang Q, Li Z, Zhang X, Bao S, Fan D, *et al.* Mesenchymal stem cells deliver and release conditionally replicative adenovirus depending on hepatic differentiation to eliminate hepatocellular carcinoma cells specifically. *Cancer letters* **2016**;381(1):85-95.
19. Moreno R, Rojas LA, Villellas FV, Soriano VC, Garcia-Castro J, Fajardo CA, *et al.* Human Menstrual Blood-Derived Mesenchymal Stem Cells as Potential Cell Carriers for Oncolytic Adenovirus. *Stem cells international* **2017**;2017:3615729.
20. Rojas JJ, Guedan S, Searle PF, Martinez-Quintanilla J, Gil-Hoyos R, Alcayaga-Miranda F, *et al.* Minimal RB-responsive E1A promoter modification to attain potency, selectivity, and transgene-arming capacity in oncolytic adenoviruses. *Molecular therapy : the journal of the American Society of Gene Therapy* **2010**;18(11):1960-71.
21. Appledorn DM, Patial S, McBride A, Godbehere S, Van Rooijen N, Parameswaran N, *et al.* Adenovirus vector-induced innate inflammatory mediators, MAPK signaling, as well as adaptive immune responses are dependent upon both TLR2 and TLR9 in vivo. *Journal of immunology* **2008**;181(3):2134-44.
22. Cerullo V, Seiler MP, Mane V, Brunetti-Pierri N, Clarke C, Bertin TK, *et al.* Toll-like receptor 9 triggers an innate immune response to helper-dependent adenoviral vectors. *Molecular therapy : the journal of the American Society of Gene Therapy* **2007**;15(2):378-85.
23. Wilson AA, Kwok LW, Porter EL, Payne JG, McElroy GS, Ohle SJ, *et al.* Lentiviral delivery of RNAi for in vivo lineage-specific modulation of gene expression in mouse lung macrophages. *Molecular therapy : the journal of the American Society of Gene Therapy* **2013**;21(4):825-33.
24. Fajardo CA, Guedan S, Rojas LA, Moreno R, Arias-Badia M, de Sostoa J, *et al.* Oncolytic Adenoviral Delivery of an EGFR-Targeting T-cell Engager Improves Antitumor Efficacy. *Cancer research* **2017**;77(8):2052-63.
25. Tanoue K, Rosewell Shaw A, Watanabe N, Porter C, Rana B, Gottschalk S, *et al.* Armed Oncolytic Adenovirus-Expressing PD-L1 Mini-Body Enhances Antitumor Effects of Chimeric Antigen Receptor T Cells in Solid Tumors. *Cancer research* **2017**;77(8):2040-51.
26. Calandra T, Roger T. Macrophage migration inhibitory factor: a regulator of innate immunity. *Nature reviews Immunology* **2003**;3(10):791-800.
27. Romieu-Mourez R, Francois M, Boivin MN, Bouchentouf M, Spaner DE, Galipeau J. Cytokine modulation of TLR expression and activation in mesenchymal stromal cells leads to a proinflammatory phenotype. *Journal of immunology* **2009**;182(12):7963-73.
28. Gupta KK, Xu Z, Castellino FJ, Ploplis VA. Plasminogen activator inhibitor-1 stimulates macrophage activation through Toll-like Receptor-4. *Biochemical and biophysical research communications* **2016**;477(3):503-8.
29. Teigler JE, Kagan JC, Barouch DH. Late endosomal trafficking of alternative serotype adenovirus vaccine vectors augments antiviral innate immunity. *Journal of virology* **2014**;88(18):10354-63.
30. Zhu J, Huang X, Yang Y. Innate immune response to adenoviral vectors is mediated by both Toll-like receptor-dependent and -independent pathways. *Journal of virology* **2007**;81(7):3170-80.
31. Liu Q, Muruve DA. Molecular basis of the inflammatory response to adenovirus vectors. *Gene therapy* **2003**;10(11):935-40.
32. Lyakh LA, Koski GK, Young HA, Spence SE, Cohen PA, Rice NR. Adenovirus type 5 vectors induce dendritic cell differentiation in human CD14(+) monocytes cultured under serum-free conditions. *Blood* **2002**;99(2):600-8.

33. Ribas A, Dummer R, Puzanov I, VanderWalde A, Andtbacka RHI, Michielin O, *et al.* Oncolytic Virotherapy Promotes Intratumoral T Cell Infiltration and Improves Anti-PD-1 Immunotherapy. *Cell* **2017**;170(6):1109-19 e10.
34. Woller N, Gurlevik E, Fleischmann-Mundt B, Schumacher A, Knocke S, Kloos AM, *et al.* Viral Infection of Tumors Overcomes Resistance to PD-1-immunotherapy by Broadening Neoantigenome-directed T-cell Responses. *Molecular therapy : the journal of the American Society of Gene Therapy* **2015**;23(10):1630-40.
35. Parrish C, Scott GB, Migneco G, Scott KJ, Steele LP, Ilett E, *et al.* Oncolytic reovirus enhances rituximab-mediated antibody-dependent cellular cytotoxicity against chronic lymphocytic leukaemia. *Leukemia* **2015**;29(9):1799-810.
36. Cascallo M, Alonso MM, Rojas JJ, Perez-Gimenez A, Fueyo J, Alemany R. Systemic toxicity-efficacy profile of ICOVIR-5, a potent and selective oncolytic adenovirus based on the pRB pathway. *Molecular therapy : the journal of the American Society of Gene Therapy* **2007**;15(9):1607-15.
37. Kasono K, Blackwell JL, Douglas JT, Dmitriev I, Strong TV, Reynolds P, *et al.* Selective gene delivery to head and neck cancer cells via an integrin targeted adenoviral vector. *Clinical cancer research : an official journal of the American Association for Cancer Research* **1999**;5(9):2571-9.
38. Lee AJ, Chen B, Chew MV, Barra NG, Shenouda MM, Nham T, *et al.* Inflammatory monocytes require type I interferon receptor signaling to activate NK cells via IL-18 during a mucosal viral infection. *The Journal of experimental medicine* **2017**;214(4):1153-67.
39. Michel T, Hentges F, Zimmer J. Consequences of the crosstalk between monocytes/macrophages and natural killer cells. *Frontiers in immunology* **2012**;3:403.
40. Gasteiger G, Rudensky AY. Interactions between innate and adaptive lymphocytes. *Nature reviews Immunology* **2014**;14(9):631-9.
41. Alcayaga-Miranda F, Cuenca J, Luz-Crawford P, Aguila-Diaz C, Fernandez A, Figueroa FE, *et al.* Characterization of menstrual stem cells: angiogenic effect, migration and hematopoietic stem cell support in comparison with bone marrow mesenchymal stem cells. *Stem cell research & therapy* **2015**;6:32.
42. Darzi S, Werkmeister JA, Deane JA, Gargett CE. Identification and Characterization of Human Endometrial Mesenchymal Stem/Stromal Cells and Their Potential for Cellular Therapy. *Stem cells translational medicine* **2016**;5(9):1127-32.
43. Rodrigues MC, Lippert T, Nguyen H, Kaelber S, Sanberg PR, Borlongan CV. Menstrual Blood-Derived Stem Cells: In Vitro and In Vivo Characterization of Functional Effects. *Advances in experimental medicine and biology* **2016**;951:111-21.
44. Rodriguez-Garcia A, Gimenez-Alejandre M, Rojas JJ, Moreno R, Bazan-Peregrino M, Cascallo M, *et al.* Safety and efficacy of VCN-01, an oncolytic adenovirus combining fiber HSG-binding domain replacement with RGD and hyaluronidase expression. *Clinical cancer research : an official journal of the American Association for Cancer Research* **2015**;21(6):1406-18.
45. Eriksson E, Milenova I, Wenthe J, Stahle M, Leja-Jarblad J, Ullenhag G, *et al.* Shaping the Tumor Stroma and Sparking Immune Activation by CD40 and 4-1BB Signaling Induced by an Armed Oncolytic Virus. *Clinical cancer research : an official journal of the American Association for Cancer Research* **2017**;23(19):5846-57.
46. Tahtinen S, Blattner C, Vaha-Koskela M, Saha D, Siurala M, Parviainen S, *et al.* T-Cell Therapy Enabling Adenoviruses Coding for IL2 and TNFalpha Induce Systemic Immunomodulation in Mice With Spontaneous Melanoma. *Journal of immunotherapy* **2016**;39(9):343-54.

Figures and legends

Figure 1. Effect of oncolytic adenovirus infection on MenSCs immunophenotypic profile.

(A) MenSCs expressing TLR-9 was analyzed by flow cytometry on OAdv-infected (white) or uninfected (black) MenSCs. Bars represent the mean \pm SD of triplicates from three independent experiments. *, $P < 0.05$ by Mann-Whitney test. (B) Luciferase activity was determined from OAdv infected or uninfected MenSCs/pHAGE-NF κ B-GFP/Luc cell lysates at different time-points after infection. Bars represent the mean \pm SD of triplicates from three independent experiments. *, $P < 0.05$ by Mann-Whitney test. The supernatants from uninfected or 48h OAdv-infected MenSCs were analysed for the presence of secreted cytokines. (C) Pixel intensity quantification is shown after Proteome Profiler Human Cytokine Array analysis. IL-8, interleukin 8; MIF, Macrophage migration inhibitory factor. Bars represent the mean \pm SD of spot duplicates from two independent experiments. (D) Luminex analysis of cytokine concentration is shown. Bars represent the mean \pm SD of duplicates from two independent experiments.

Figure 2. Pro-inflammatory cytokines production in autologous or allogeneic PBMCs co-

cultures with OAdv-infected MenSCs. Uninfected or OAdv-infected (MOI = 50) MenSCs from 3 different donors were co-cultured with autologous or allogeneic human PBMCs at a PBMCs-to-MenSCs ratio of 10 in triplicates. After 48h of co-culture, culture medium was collected and cytokines level assessed by ELISA. The mean \pm SD of triplicates from two independent experiments is shown. *, $P < 0.05$; ***, $P < 0.001$ by Kruskal-Wallis with Dunn *post-hoc* test.

Figure 3. Effect of monocyte and/or NK cell depletion on pro-inflammatory cytokines production in co-cultures of OAdv-MenSCs and allogeneic PBMCs. Allogeneic human PBMCs from the same donor were depleted for monocytes and/or NK cells, and co-cultured with uninfected or OAdv-infected MenSCs (PBMCs:MenSC =10). Non-depleted PBMCs alone or in co-culture with OAdv-infected MenSCs were used as control. After 48h of co-culture, culture medium was collected and cytokines level assessed by ELISA. The mean \pm SD of triplicates from two independent experiments is shown. *, P< 0.05; **, P< 0.01; ***, P< 0.001 by Kruskal-Wallis with Dunn *post-hoc* test.

Figure 4. CD4⁺ CD8⁺ T-cell and NK-cell activation in co-cultures of autologous or allogeneic human PBMCs with OAdv-infected MenSCs. Uninfected or OAdv-infected MenSCs were co-cultured with autologous or allogeneic human PBMCs at a PBMCs-to-MenSCs ratio of 10 in triplicates. After 48h of co-culture, PBMCs were harvested and T cells and NK cells analyzed. **(A)** Upper, analysis of CD69 expression. Left, example of CD4⁺ and CD8⁺ positive cells expressing CD69 histograms in different co-culture conditions. Middle, percentage of CD4⁺ and CD8⁺ positive cells expressing CD69. Right, CD69 mean fluorescent intensity of CD4⁺ and CD8⁺ positive cells. Lower, analysis of CD25 expression. Left, example of CD4⁺ and CD8⁺ positive cells expressing CD25 histograms in different co-culture conditions. Middle, percentage of CD4⁺ (left) and CD8⁺ (right) positive cells expressing CD25. Right, CD25 mean fluorescent intensity of CD4⁺ and CD8⁺ positive cells. **(B)** Upper, analysis of CD69 expression. Left, example of CD56⁺CD16⁺ positive cells expressing CD69 histograms in different co-culture conditions. Middle, percentage of CD56⁺CD16⁺ positive cells expressing CD69. Right, CD69 mean fluorescent intensity of CD56⁺CD16⁺ positive cells. Lower, analysis of CD107a expression. Left, example of CD56⁺CD16⁺ positive cells expressing CD107a histograms in

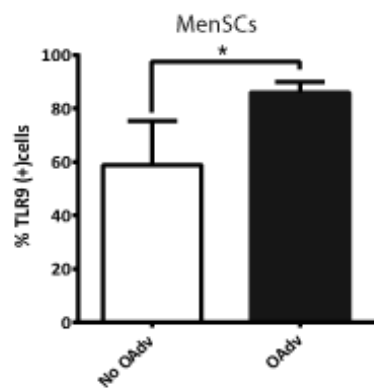
different co-culture conditions. Middle, percentage of CD56⁺CD16⁺ positive cells expressing CD107a. Right, CD107a mean fluorescent intensity of CD56⁺CD16⁺ positive cells. (C) Same experiment was performed allowing direct cell contact or using transwells system to separate OAdv-MenSCs from allogeneic PBMCs. The percentage of CD4⁺, CD8⁺ or CD56⁺CD16⁺ positive cells expressing CD69 is represented. The mean \pm SD of triplicates from two independent experiments is shown in all analysis. *, P< 0.05; **, P< 0.01, ***, P<0.001 by Kruskal-Wallis with Dunn *post-hoc* test.

Figure 5. Antitumor efficacy of OAdv-loaded MenSCs *in vitro*. A431-GL and FaDu-GL cancer cell lines were co-cultured with OAdv-infected or un-infected MenSCs in the presence or absence of allogeneic PBMCs (PBMCs:cancer cell ratio = 10) in triplicates. After 5 days in co-culture, live cancer cells were counted by flow cytometer. Cytotoxicity was expressed as the percentage of live cancer cells on co-cultures, normalized to the number of cancer cells cultured alone. *, P< 0.05; by Kruskal-Wallis with Dunn *post-hoc* test. Results from two independent experiments is shown.

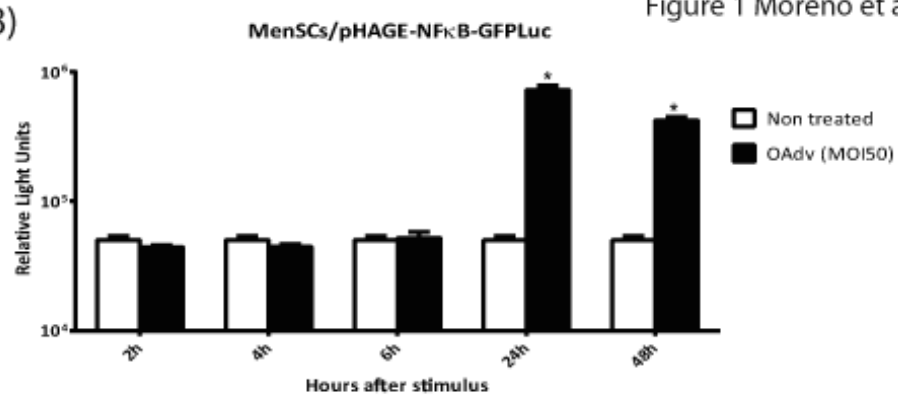
Figure 6. Antitumor efficacy of OAdv-loaded MenSCs *in vivo*. (A) Athymic nu/nu mice bearing subcutaneous A549 tumors were intraperitoneally injected with PBS, MenSCs, OAdv or MenSCs previously infected with OAdv (n=7 mice per group). Left, the mean of tumor growth \pm SEM is shown. *, P< 0.05, **, P< 0.01, ***, P<0.001 OAdv versus PBS group; #, P< 0.05 OAdv versus MenSCs; &, P< 0.05 OAdv versus MenSCs/OAdv group by Kruskal-Wallis with Dunn *post-hoc* test. Right, the presence of OAdv genomes in tumors at the end of the experiment was assessed by real-time PCR. (B) NSG mice bearing subcutaneous A549 tumors received an intravenous injection of human allogeneic PBMCs except one group (n=7 mice per group). Next

day, mice were intraperitoneally injected with PBS, MenSCs, OAdv or MenSCs previously infected with OAdv. Left, the mean of tumor growth \pm SEM is shown. *, $P < 0.05$, **, $P < 0.01$ allogeneic PBMCs+MenSC/OAdv versus PBS group by Kruskal-Wallis with Dunn *post-hoc* test. Right, the presence of OAdv genomes in tumors at the end of the experiment was assessed by real-time. Bottom panel, immunohistochemical staining of E1A of a representative tumor from each group is shown. The arrow points to positive virus E1A staining. (C) NSG mice bearing subcutaneous A431 tumors were treated as previously described. The mean of tumor growth \pm SEM is shown. *, $P < 0.05$, **, $P < 0.01$ allogeneic PBMCs+MenSC/OAdv versus PBS group; #, $P < 0.05$ allogeneic PBMCs+MenSC/OAdv versus MenSCs; &, $P < 0.05$, allogeneic PBMCs+MenSC/OAdv versus OAdv group, by Kruskal-Wallis with Dunn *post-hoc* test. (D) NSG mice bearing subcutaneous A549 tumors received an intravenous injection of human allogeneic PBMCs or PBMCs previously depleted for monocytes or NK cells (n=7 mice per group). Next day, mice were intraperitoneally injected with PBS, or MenSCs previously infected with OAdv. Right, the mean of tumor growth \pm SEM is shown. #, $P < 0.05$, allogeneic PBMCs+MenSC/OAdv versus allogeneic PBMCs-NK⁻+MenSC/OAdv group; &, $P < 0.05$, allogeneic PBMCs+MenSC/OAdv versus allogeneic PBMCs-Mo⁻+MenSC/OAdv group by Kruskal-Wallis with Dunn *post-hoc* test. Left, analysis of the percentage of CD56⁺ cells and CD14⁺ cells in PBMC and NK or monocytes-depleted PBMCs samples respectively.

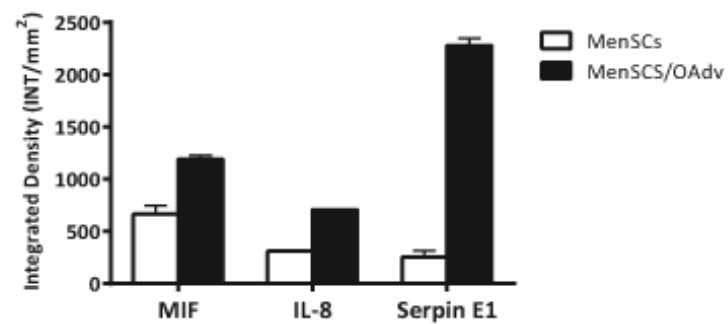
A)



B)



C)



D)

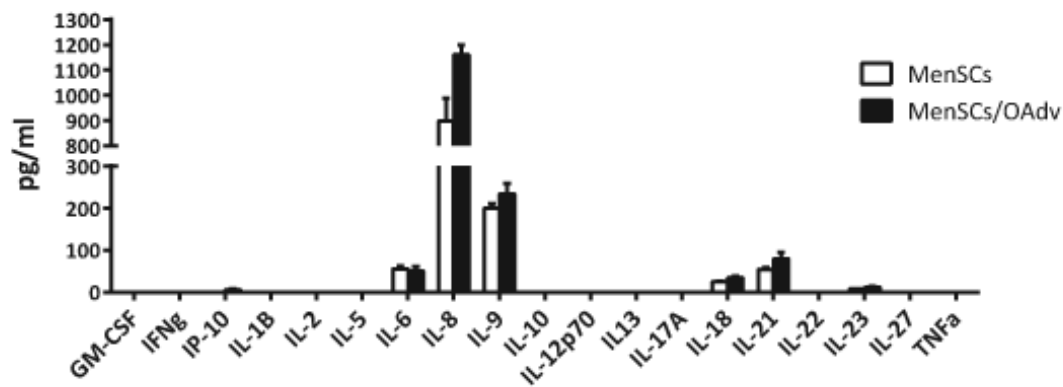


Figure 2 Moreno et al

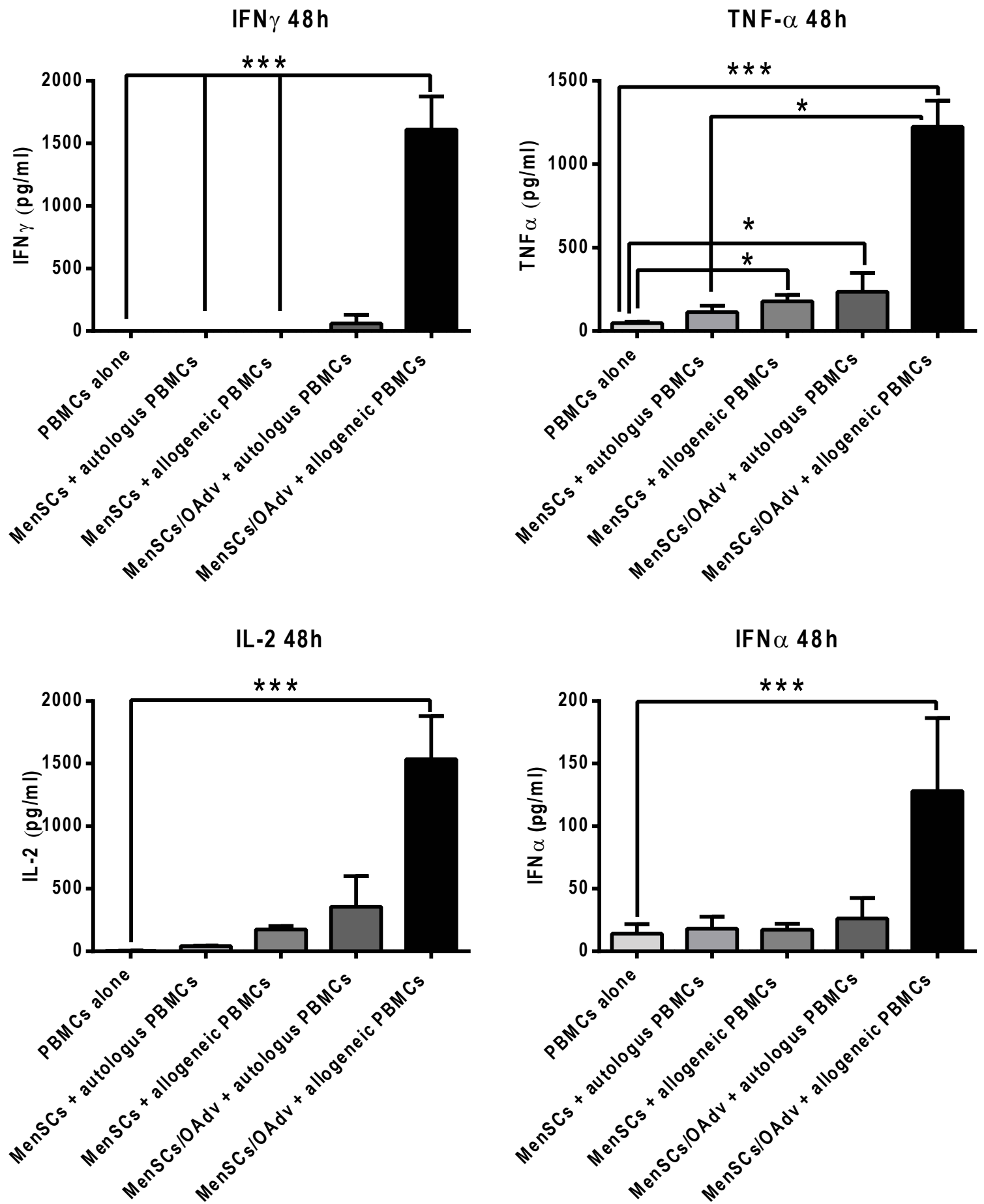
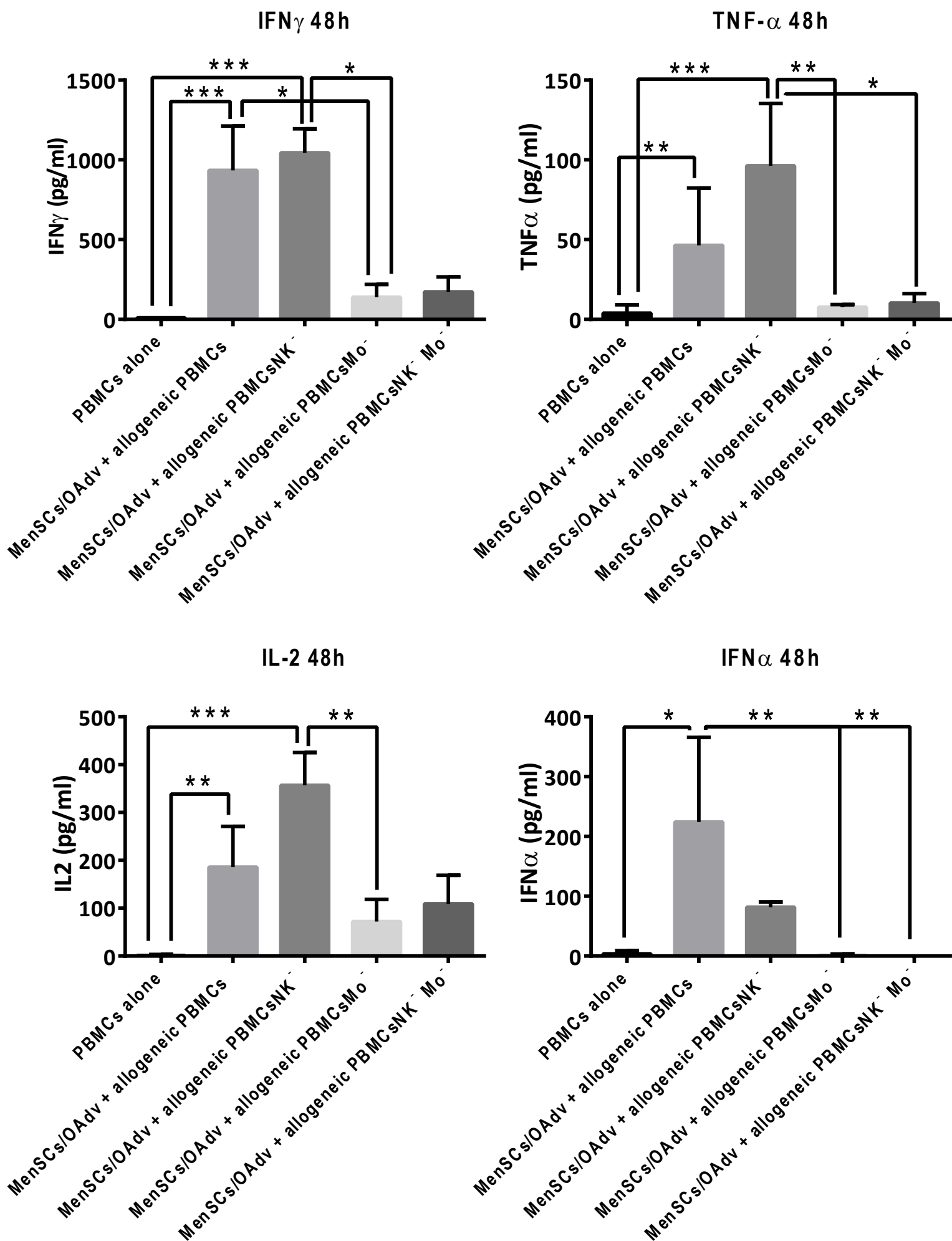


Figure 3 Moreno et al



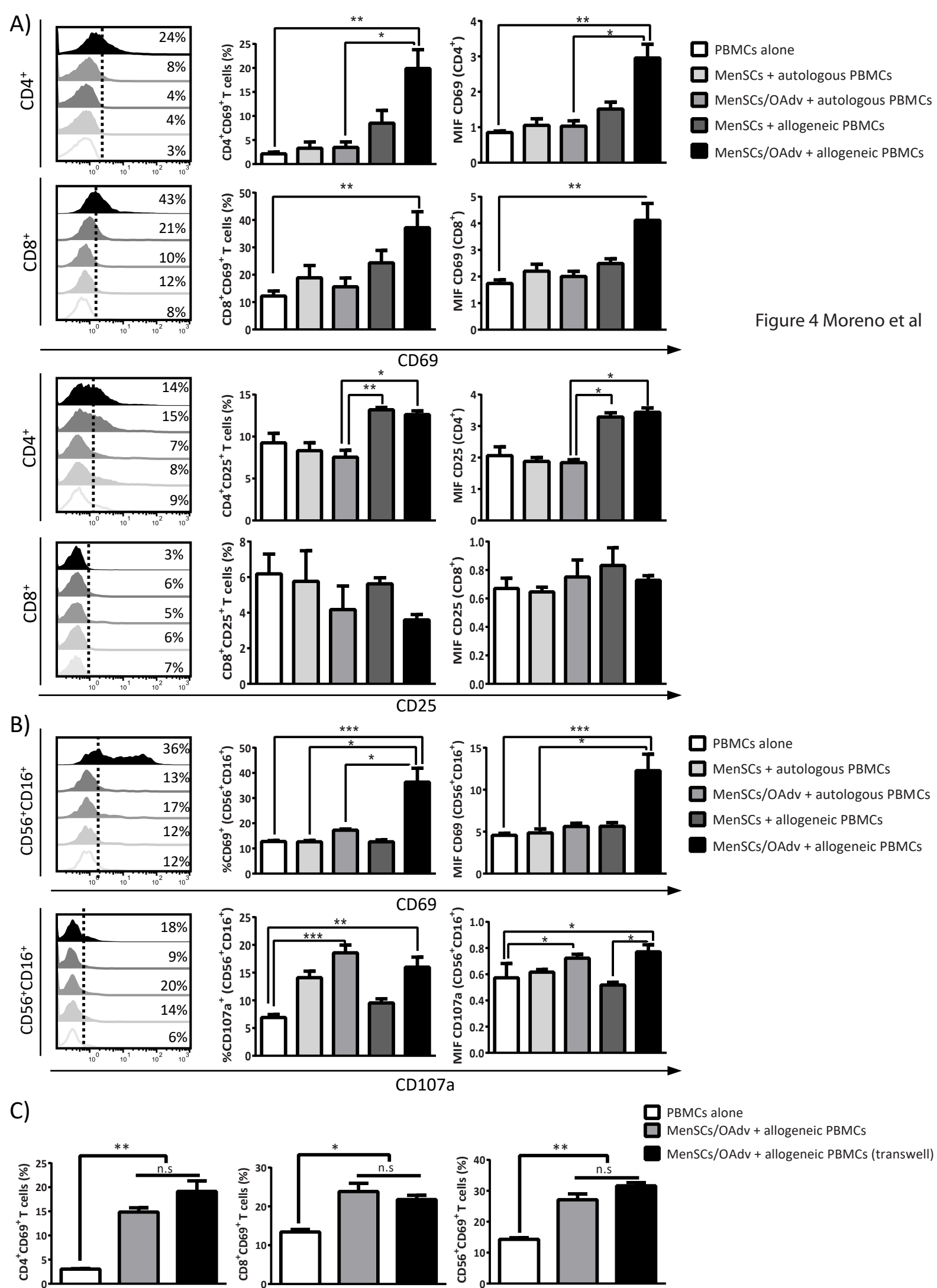
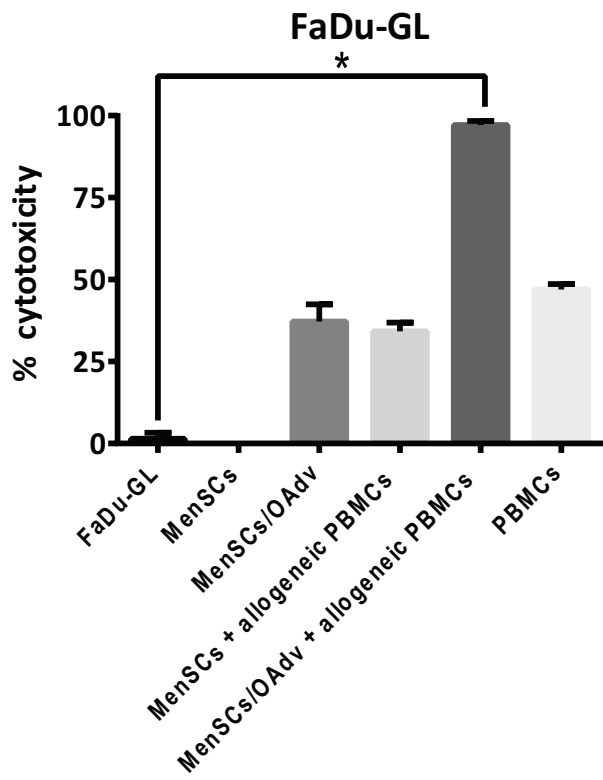
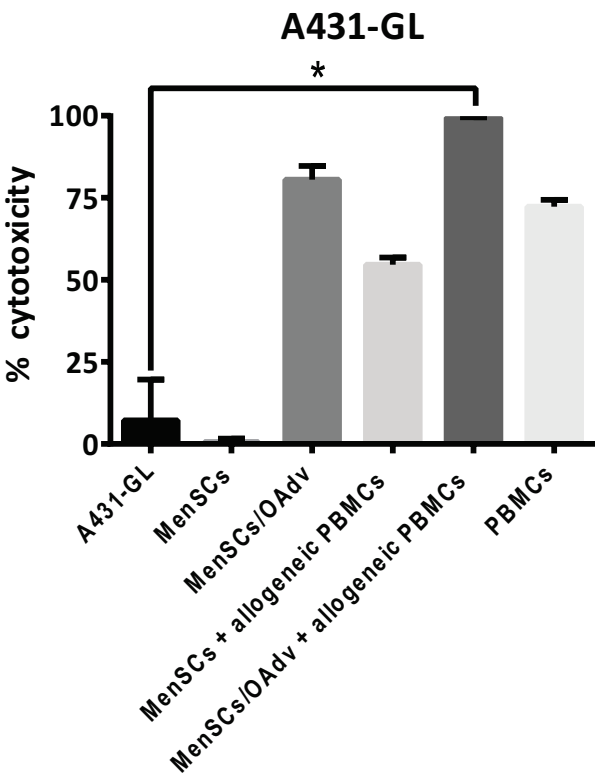
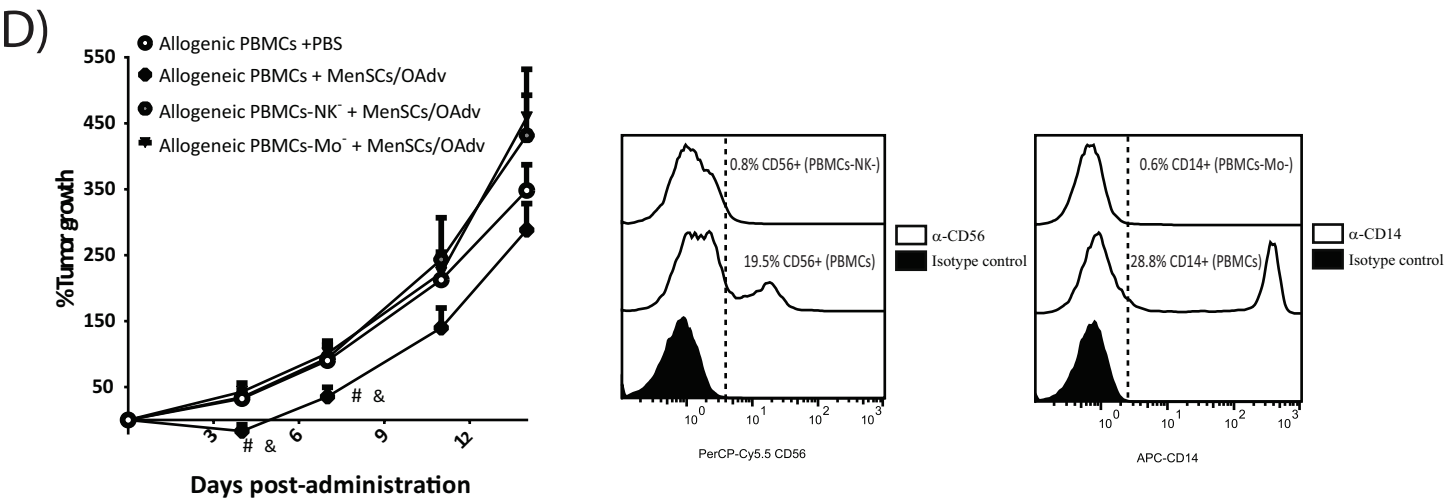
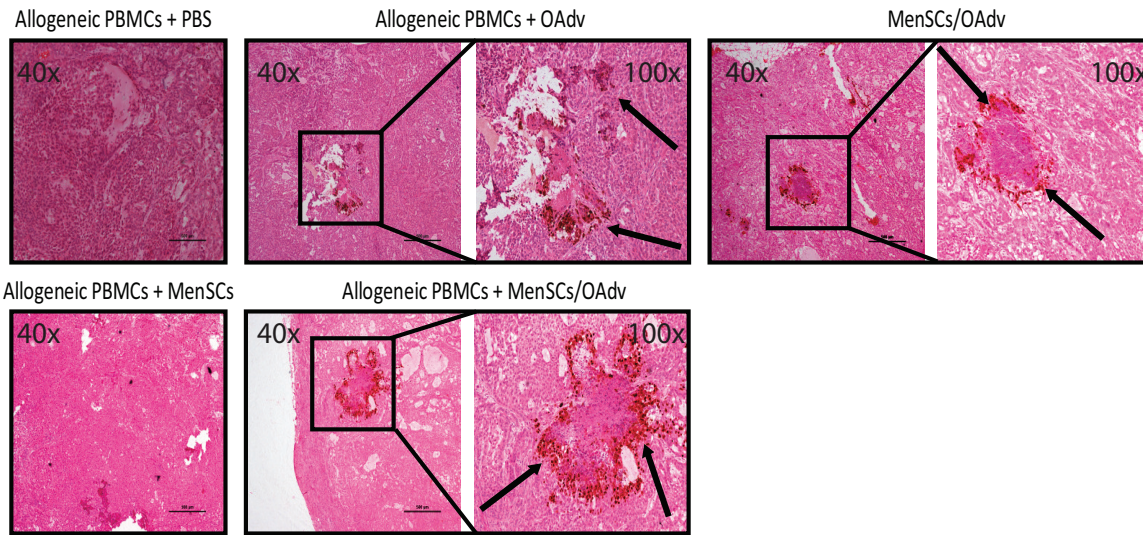
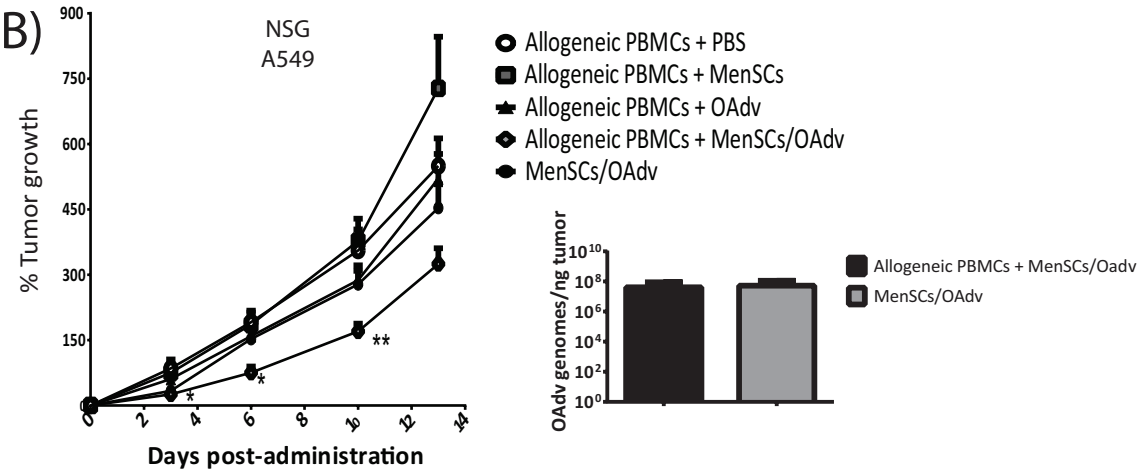
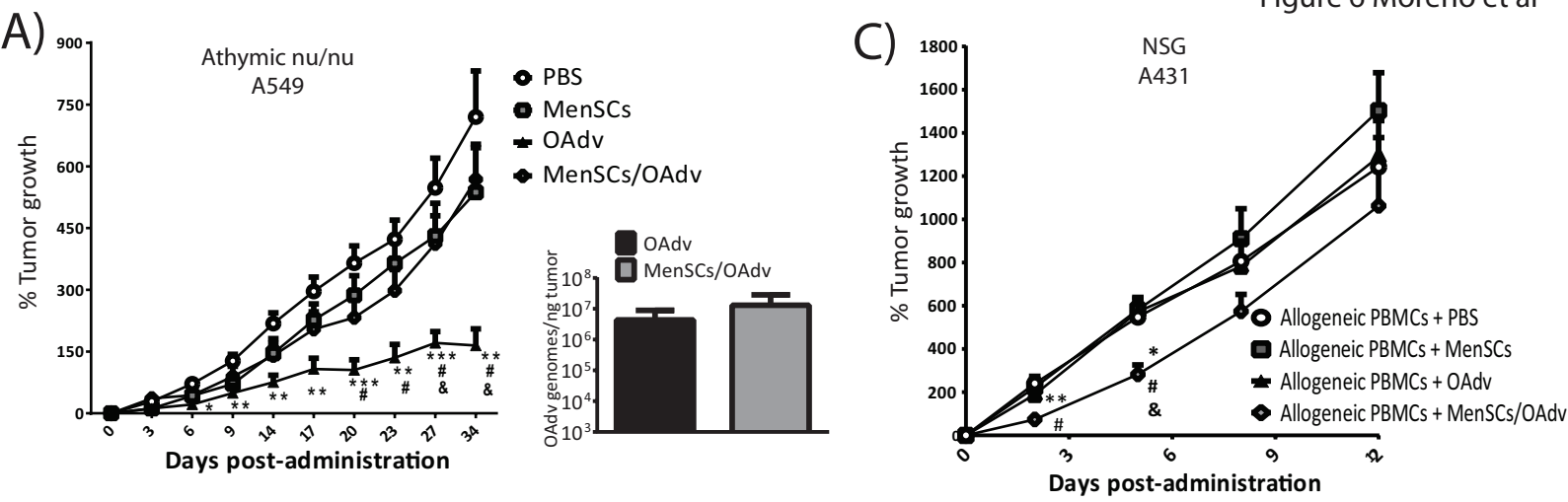


Figure 4 Moreno et al





SUPPLEMENTARY MATERIALS AND METHODS

Flow cytometry analysis of PBMC activation.

Panel 1 (T-cell activation): PE-CD4 (Biolegend, clone OKT4), V500-CD8 (BD Biosciences, San Jose, CA, USA, clone RPA-T8), APC-CD25 (Biolegend, clone BC96), and Pe-Cy7-CD69 (BD Biosciences, clone FN5U). Panel 2 (NK cell activation) PE-CD56 (BD Biosciences, clone B159); V500-CD16 (BD Biosciences, clone 3G8) Pe-Cy7-CD69 (BD Biosciences, clone FN5U), and BV421-CD107a (BD Biosciences, clone H4A3) antibodies for flow cytometer quantification. The corresponding fluorescent, isotype-matched negative control antibodies defined the background staining.

RNA interference

A lentivirus vector harboring a shRNA expression cassette against human TLR-9 (LV-shTLR9) was kindly provided by Dr. Kremmer (13). MenSCs from 3 different donors (passage 3) and MenSCs/pHAGE-NFkB-GFP_{Luc} were transduced with LV-shTLR9. shRNA knockdown efficacy was confirmed by Quantitative Real Time-PCR (qRT-PCR).

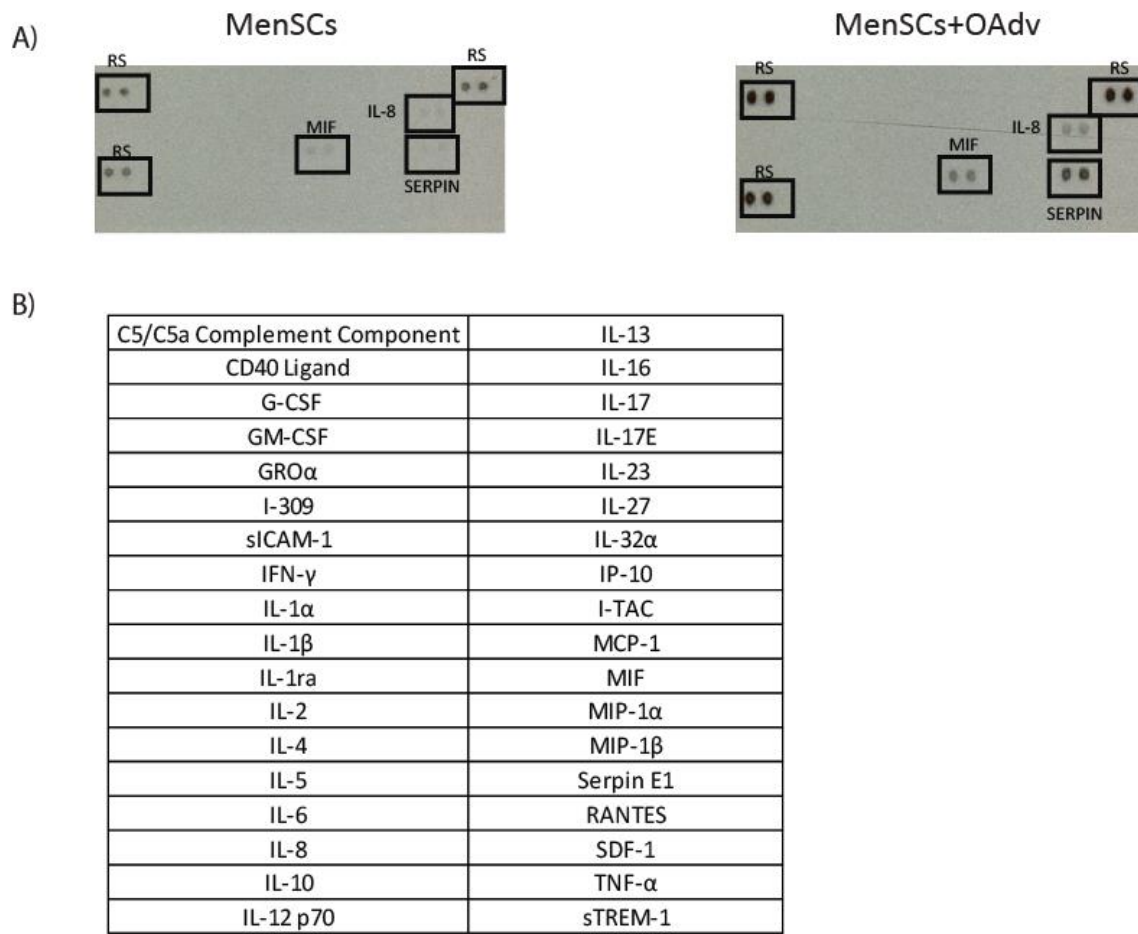
Gene-expression analysis by RT-PCR

Quantitative RT-PCR was used to analyze TLR-9, MIF, IL-8, and Serpin E1 expression. RNA from frozen OAd-infected or uninfected MenSCs and MenSCs/pHAGE-NFkB-GFP_{Luc} cell pellets was extracted with a DNA/RNA/Protein extraction kit (IBI Scientific, Peosta, IA, USA), and treated with Turbo DNA-free (Thermo Scientific) to remove genomic DNA. RNA (1µg) was reverse transcribed with the PrimeScript RT reagent kit (Takara Bio, Shiga, Japan), according to the manufacturer's instructions. qRT-PCR was performed using the LightCycler 480 SYBR Green I Master (Roche, Basel, Switzerland) in a LightCycler® 480 II machine (Roche) and analyzed with the LightCycler® 480 Software release 1.5.0 SP4 (Roche). The following primers were used:

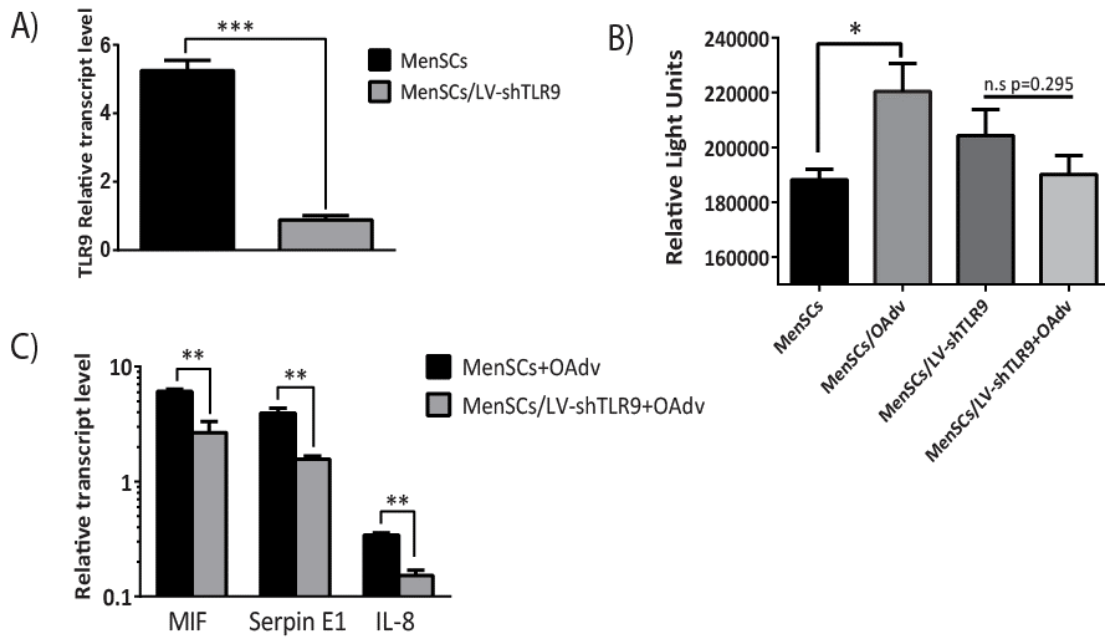
TLR9F: 5'-CCGTGACAATTACCTGGCCTTC-3 and TLR9R: 5'-

CAGGGCCTTCAGCTGGTTTC-3' for human TLR-9; MIFF: 5'-CGCAGAACCGCTCCTACAG-3' and MIFR:5'-GGAGTTGTTCCAGCCCACAT-3' for human MIF; IL8F: 5'-TTTTGCCAAGGAGTGCTAAAGA-3' and IL8R: 5'-AACCTCTGCACCCAGTTTTTC-3' for human IL-8; SerpinE1F: 5'-TCAAAACACAACCTTCTCAGTGTCATC-3' and SerpinE1R: 5'-AGCTTGCAACATAACCAGATATTGC-3'; and B-ActinF: 5'-CTGGAACGGTGAAGGTGACA-3' and B-ActinR: 5'-GGGAGAGGACTGGGCCATT-3' for human β -Actin. PCR conditions were: an activation cycle (95°C, 10minutes) followed by 40 amplification cycles (95°C 15 seconds, 60°C 1 minute and 72°C 7 seconds). Target gene expression was calculated by the $2^{-\Delta\Delta CT}$ method for relative quantification after normalization to β -actin expression.

Supplementary Figure 1 Moreno et al



Supplementary Figure 1. Cytokine array. Proteome Profiler Human Cytokine Array Kit. **(A)** A direct visualization of spots is shown. RS, reference spots; IL-8, interleukin 8; MIF, Macrophage migration inhibitory factor. **(B)** List of the 36 cytokines analyzed.



Supplementary Figure 2. Effect of TLR-9 knock-down on OAd-infected MenSCs

properties. (A) qRT-PCR to detect relative expression of TLR-9 from three different MenSCs donors, untreated or infected with a lentivirus coding for a small hairpin-RNA against the human TLR-9. The mean \pm SD from two independent experiments is shown. ***, $P < 0.001$ by Mann-Whitney test. (B) Luciferase activity from normal or TLR-9 down-regulated MenSCs \pm OAdv cell lysates was determined 48h after infection. Whereas a significant increase of luminescence signal was detected when MenSCs/pHAGE-NFKB-GFP_{Luc} were infected with the OAdv, the signal coming from MenSCs/pHAGE-NFKB-GFP_{Luc} treated with the LV-shTLR-9 did not change after OAdv infection. Bars represent the mean \pm SD of triplicates from two independent experiments. *, $P < 0.05$ by Mann-Whitney test. (C) qRT-PCR to detect the relative expression of MIF, Serpin E1, and IL-8 from three different MenSCs donors, untreated or infected with a lentivirus coding for a small hairpin-RNA against the human TLR-9. A reduction in the relative transcript levels of MIF, Serpin E1, and IL-8 were observed in OAd-infected MenSCs after TLR-9 down-regulation. The mean \pm SD from two independent experiments is

shown. **, $P < 0.01$ by Mann-Whitney test.